ANALYSIS AND RECOVERY OF SYSTEMATIC ERRORS IN AIRBORNE LASER SYSTEM

Zhihe Wang*, Rong Shu ,Weiming Xu, Hongyi Pu, Bo Yao

Shanghai Institute of Technical Physics, CAS, 500 Yutian Road, Shanghai 200083, P. R. of China – zhhwang@mail.sitp.ac.cn

Commission VI, ICWG V/I

KEY WORDS: Airborne laser system, System errors, Error recovery, adjustment model, Surface extraction

ABSTRACT:

Although some mature manufactures of airborne laser system (ALS) have been published for some years, however, in china, the development of ALS just is on the starting step. Shanghai Institute of Technical Physics (SITP), CAS is developing a new airborne laser instrument. It is the best difficult task to determining the systematic biases of ALS. The ultimate goal is to determine the master systematic errors and to correct the raw laser points. By analyzing the systematic error source firstly, the adjustment model presented in paper enable modelling and removing the actual errors in laser point sets. Interesting surfaces and regions can be determined by a least-squares plane fit through a subset of laser points. The proposal model of solution is based on integrating the observations and adequate control planes and the redundancy in the overlapping areas of laser data sets. It has been demonstrated that moderate slopes are sufficient to generate reliable solutions. In addition, the precision of ranging and scan angle aiming to the same target point is tested by laboratory experiment at the end of paper.

1. INTRODUCTION

Although some mature manufactures of airborne laser scanning (ALS) have been published for some years, however, in china, the development of ALS just is on the starting step. Shanghai Institute of Technical Physics (SITP), CAS is developing a new airborne laser instrument. Its laser pulse rates have achieved 50k Hz and its scan rates have 40 Hz. It is capable of recording multi return signal instead of either the first or the last return. It provides a 3D point cloud as a primary product. The achievements in developing appropriate ALS data processing software, however, have been rather marginal.

It is the best difficult task to determining the systematic biases of ALS. The ultimate goal is to determine the master systematic errors and to correct the raw laser points such that only random errors are left. The factors affecting laser-target position accuracy are numerous. Huising and Gomes Pereira (1998) report about systematic errors of 20 cm in elevation and of several meters in position between overlapping laser strips, Crombaghs et al. (2000) identify systematic trends between overlapping strips.

Apart from the target reflectivity properties and laser-beam incidence angle, the main limiting factors are the accuracy of the platform position and orientation derived from the carrier-phase differential GPS/INS data and uncompensated effects in system calibration. The calibration can be divided into that of calibration of individual sensors such as the laser range-finder and that concerning spatial (lever-arm) or orientation (bore-sight) offsets between the sensors due to a particular assembly. In most system installations, the lever-arms between LiDAR-IMU-GPS sensors can be determined separately by independent means, although this represents certain difficulties related to the realization of the IMU body frame. On the other hand, the determination of the bore-sight angles is only possible in-flight once the GPS/INS-derived orientation becomes sufficiently accurate.

The existing calibration procedures, while functional, are recognized as being sub-optimal since they are labor-intensive (i.e., they require manual procedures), non-rigorous and provide no statistical quality assurance measures. Furthermore, the existing methods often cannot reliably recover all three of the angular mounting parameters. The problem is worsened by the angular uncertainty due to the broad laser beam width (Lichti, 2004). On the other hand, the cross-section method seems to be popular in commercial systems and usually provides satisfactory results for the bore-sight estimate in the roll direction. However, its use for the recovery of pitch and yaw/heading direction is less appropriate. The use of the slope gradients in DTM/DSM for bore-sight estimation made its way to a popular software package used for ALS data handling (Soininen and Burman, 2005). The principal weakness of this approach is the strong correlation of the bore-sight angles with unknown terrain shape. Also, the implemented stochastic model of the LiDAR trajectory assumes time-invariant behavior of the GPS/INS errors that is not realistic.

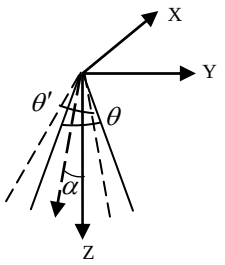

Figure 1. Illustration of scan angle errors

The organization of the paper is as follows. At the first, definition of system errors and their influence with respect to mapping results are described. The paper focuses on the proposed error model, and its linearization is presented. The subsequent discussion concerns the recovery of the main error parameters such as range error and bore-sight angles and the analysis of control and tie information. Finally, paper provides a brief summary, and an outlook for further work.

2. ERROR SOURCES

Generally speaking, there are three types of errors during a process of measurement: blunders, systematic biases and random errors. Blunders are significantly larger than the other two types. They can be easy detected and eliminated with use of empirical parameters. Random errors are always present and can never be eliminated, however, can be minimized by least-square solution and redundant observations. As to systematic errors, they are caused by imperfect instruments. They can be represented through some parameters, which are estimated by a mathematic model from redundant observations. The type of errors including range error, scan angle errors, bore-sight angles and level arms from the INS system to the laser local coordinate system are emphatically discussed in this section.

2.1 Range Error and Scan Angle Errors

The ranging measurement is determining the time-of-flight of a light pulse, i.e., by measuring the travelling time between the emitted and the received pulse. Various factors contribute to the range error. It has relation with not only optical and electronical designment but also target reflectivity because range accuracy is inversely proportional to the square root of the signal-to-noise ratio(S/N).The S/N lie on many factors, such as power of emitted and received signal, input bandwidth, background radiation, responsivity of the signal detector, etc. Furthermore, if airplane flies on rather a better altitude as 2000 m, range error is dependent on the atmospheric disturbances because of variability of atmospheric refractive index. For simplicity, herein, it is regarded as unknown small constant.

Scan angle errors are depicted in Fig.1 The ideal system is systemtric to the z-axis with a scan angle θ. The real scanning system is rotated by the alignment error α and the scan angle is θ'. It chiefly includes the following three error sources:

Alignment error α the zero degree direction (broken line Z-axis) and the plumb line (real line Z-axis) may not coincide. The angle bias α is amounted to adding a constant angle k to scan angle.

Scan angle error $\Delta\theta$ an inaccurate scan angle affect scan angle. It does not suffer from non-linear effects and is therefore omitted.

Scan plane error expresses that the scan plane and the X-axis are not perpendicular. The offset is described by the two exceeding small angular errors. So it is omitted as well as.

The alignment angle influences on the mapping result more than the latter two errors. Therefore, we contribute the alignment angle to error model. These errors result to non-linear effect to the laser points position, in particular, at the end of the swath as the reported paper(Crombaghs,2000).

2.2 Bore-sight Angles and Level-arm Vector

Considering mounting errors of the laser scanning (LS) sensor with respect to the INS sensor, the LS and INS coordinate system are not parallel. The alignment error is expressed by the small rotation matrix. The bore-sight angles are the main aim of the recovery system errors because they are determined well by other means. Therefore, the bore-sight angles must be estimated more precisely during an in-flight calibration procedure. The practical influence of the bore-sight on the mapping result is demonstrated by Fig. 2. This figure shows a cross-section of a building. It is illustrated with the profile that the discrepancies due to bore-sight angles are clearly visible on the inclined planes.

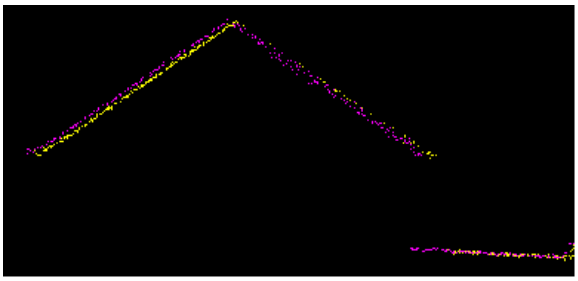

Figure 2. Effect of bore-sight errors on a cross-section profile of a building roof from 2 flight lines of different directions and heights

The magnitude of the lever-arm vector between LS and INS origins can be measured quite accurately. It is usually neglected. As for the lever-arm vector between the center of GPS antenna and INS origins, the measuring accuracy can achieve to the level of cm after installation on the ground. As mention above, if the bore-sight angles are considerably larger, the level-arm vector is thus not as accurate as its magnitude, so larger level-arm quantities may be expected, i.e., they can not be omitted. There errors exhibit to some extent linear effect to the laser points (Crombaghs,2000).

2.3 INS Errors and GPS Errors

INS errors are derived from shift or drift of INS sensor. GPS errors are caused by some factors such as differential troposphere, ionosphere delay, multipath and clock biases, etc.. Certainly, they are contributing to the mapping accuracy and are determined as estimated parameters added to the adjusting model (Filin and Vosselman, 2004). However, it is difficult to estimate these, and even the quality of the unknown parameters estimates may be degraded as additional correlation. At present, the POSPAC software of version 4.4 produced by APPLANIX company can implement the difference of GPS based on multi-base Kalman Filter and integrated inertial navigation and smoothing optimization, which achieve a level that the residual effect in GPS/INS trajectory estimation are lower than 0.05m and 0.005° in position and attitude respectively under the optimization of the calibration area and the flight conditions. Fig.3 depicts the position RMS error derived from GPS/INS processing by POSPAC software. So the additional parameters of INS and GPS biases are not added to the estimated model.

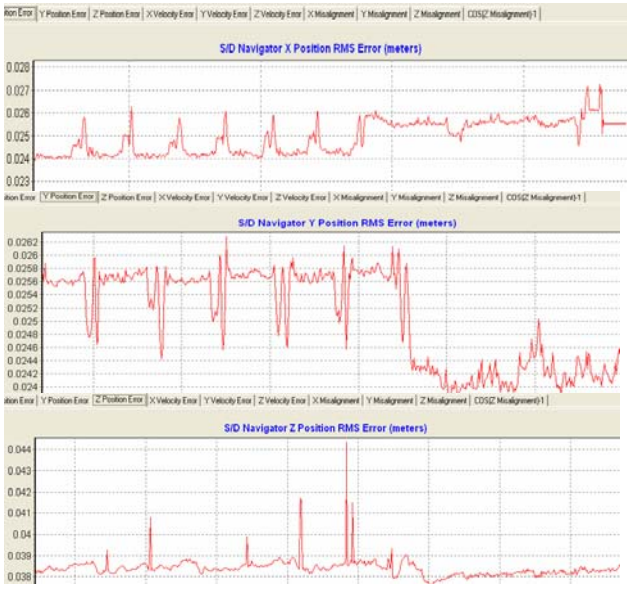

Figure 3. Navigator position RMS for X, Y, and Z direction

3. ERROR REVOERY MODEL

3.1 Geo-Referencing of LiDAR Measurements

As already mentioned, it is necessary to compute the laser point geo-referencing that represent mathematical models. The geo-referencing of the laser points is viewed as a function of the observation from the above parameters estimated. The LiDAR geo-referencing equation in a local reference frame can be given in eq.1:

$$\begin{bmatrix} x_l \\ y_l \\ z_l \end{bmatrix}^m = \begin{bmatrix} X \\ Y \\ Z \end{bmatrix}^m + R_{imu}^m \left(\begin{bmatrix} \Delta x \\ \Delta y \\ \Delta z \end{bmatrix} + R_m Rs \begin{bmatrix} 0 \\ 0 \\ \rho \end{bmatrix} \right) \quad (1)$$

where:

x_l, y_l, z_l =the laser footprint position in the mapping frame

X, Y, Z =position of the phase center of GPS antenna in the mapping frame

$\Delta x, \Delta y, \Delta z$ =ever arm vector from the phase center of GPS antenna to laser scanner center

R_{imu}^m =the rotate matrix between the IMU frame and the mapping frame described by roll, pitch and yaw observation

R_m =a priori known rotation matrix from the IMU frame to the LS coordinate frame that depends on the mounting situation.

$R_S = \begin{bmatrix} 1 & 0 & 0 \\ 0 & \cos\theta & -\sin\theta \\ 0 & \sin\theta & \cos\theta \end{bmatrix}$ =laser scanner rotation

θ =the LiDAR encoder angular value

ρ =the LiDAR range at time t

3.2 Recovery Function Model

The following model is based on constraining the target objects to the surface extracted from the laser points and known knowledge as planes, slopes. Some factors of there unknown planes are estimated together with the calibration parameters. The parameters of a plane j are described as

$$\vec{S}_j = \begin{bmatrix} S_{1j} & S_{2j} & S_{3j} & S_{4j} \end{bmatrix}^T \quad (2)$$

where S_1, S_2 and S_3 are the direction cosines of the plane's normal vector and S_4 is the negative orthogonal distance between the plane and the coordinate system origin. The observation equation for an point i expressed by its coordinates x_i, y_i, z_i lying on plane j has the form

$$s_{1j}x_i + s_{2j}y_i + s_{3j}z_i + s_{4j} = 0 \quad (3)$$

Note that the direction cosines must satisfy the following unit length constraint

$$s_{1j}^2 + s_{2j}^2 + s_{3j}^2 = 1 \quad (4)$$

Combining equation (1) with equation (2) consist of the form that constraint conditions and laser points position as a function of the systematic errors:

$$F(O, X) = 0 \quad (5)$$

where, O is the observations, X is the systematic errors.

The geo-referencing of the laser points in the laser coordination system is viewed as a function of the GPS, INS, range, scan-angle, and the systematic biases. In section 2, the systematic biases are selected from bore-sight angles, ranging biases, and scanning angle biases. After adding the systematic errors to the equation (1), the geo-referencing of the laser points is changed by the following form:

$$\begin{bmatrix} x \\ y \\ z \end{bmatrix}^m = \begin{bmatrix} X \\ Y \\ Z \end{bmatrix}^m + R_{imu}^m \left(\begin{bmatrix} \Delta x \\ \Delta y \\ \Delta z \end{bmatrix} + \Delta R_m R_m \Delta R_s R_s \begin{bmatrix} 0 \\ 0 \\ \rho + \Delta\rho \end{bmatrix} \right) \quad (6)$$

with

$\Delta\rho$ =the range bias

ΔR_s =rotation matrix with alignment error α defined in section 2

$\Delta R_m = \begin{bmatrix} 1 & -\kappa & -\varphi \\ \kappa & 1 & -\omega \\ \varphi & \omega & 1 \end{bmatrix}$ =bore-sight rotation matrix

ω, φ, κ =bore-sight angles

Since the equation (6) is non-linear and each laser point position is represented by more than one observation, the adjustment model must be used. Substituting the equation (6) to

the equation (5), the linearized form of equation (5) is given in Eq.7.

$$B\hat{x} + Av + w = 0 \tag{7}$$

where B is partial matrix with respect to unknowns, namely the calibration parameters; A is partial matrix with respect to observations; $\hat{X}$ is vector of unknowns; V is the vector of residuals; W is the misclosure vector, i.e. the equation (5) evaluated at current estimate of the parameters and observations

The solution of equation (7) is adopted by the traditional approach of least-squares adjustment. Namely, the sum of weighted squares of the residuals reaches minimization. Following standard procedures, the resulting final form of the normal equations used herein is:

$$\hat{x} = (B^T (AC_{vv}A^T)^{-1} B)^{-1} B^T (AC_{vv}A^T)^{-1} w \tag{8}$$

with:

$$\hat{\sigma}_0^2 = \frac{(Av)^T (AC_{vv}A^T)^{-1}(Av)}{n-m} \tag{9}$$

$$\hat{D}_{\hat{x}\hat{x}} = \hat{\sigma}_0^2 (B^T (AC_{vv}A^T)^{-1} B)^{-1} \tag{10}$$

where $\hat{\sigma}_0^2$ the variance component; C_{vv} the covariance matrix of observation; n the number of target laser points; m the number of unknowns.

3.3 Surface Extraction

For the strip adjustment, surfaces are the natural candidates to be used. The selecting areas are suitable for the adjustment and improve the estimation of the parameters. For the effect of noise on the surface parameters, artifacts are introduced into the observation. The surface model is, therefore, used in the form a surface constraint in equation (3). Interesting surfaces and regions can be determined by a least-squares plane fit through a subset of laser points. The extraction procedure that is used herein is based on minimizing the weighted quadratic sum of the distances of the laser points to the plane (Lee, Schenk 2001).

The standard deviation of unit weight σ_0 can, therefore, be interpreted as the standard deviation σ_D of the shortest distance of a point to the plane. The plane is accepted if σ_0 is smaller than, or equals, a threshold. Experience shows that most of significant surface have a std. small than 15 cm. The threshold is the average standard deviation of the distances to the plane computed by error propagation from the standard deviations of the laser point positions tested for the plane fit. For a horizontal plane it is just a function of the z-components, and thus influenced only by the accuracy in z. The steeper the slope of the plane, however, the greater will be the effect of the x and y planimetric components. If a plane is accepted, the neighboring points are tested statistically for the fit to the plane. If the fitting error remains smaller than the given threshold, the points are used to update the plane parameters using sequential least-squares. Figure 6 to 7 show examples for extracting surface.

In Fig.6, red points represent the each planes of the building. In Fig.7, the central region is extracted as well as, but don't split up the bottom plane.

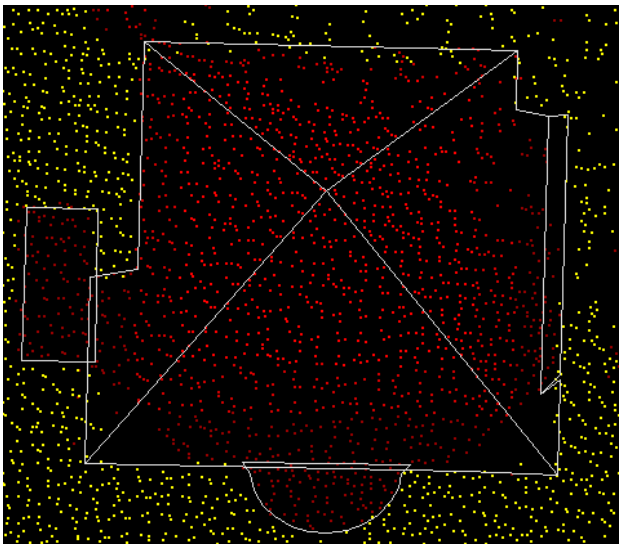

Figure 6. Points of extracted slope surface for a building

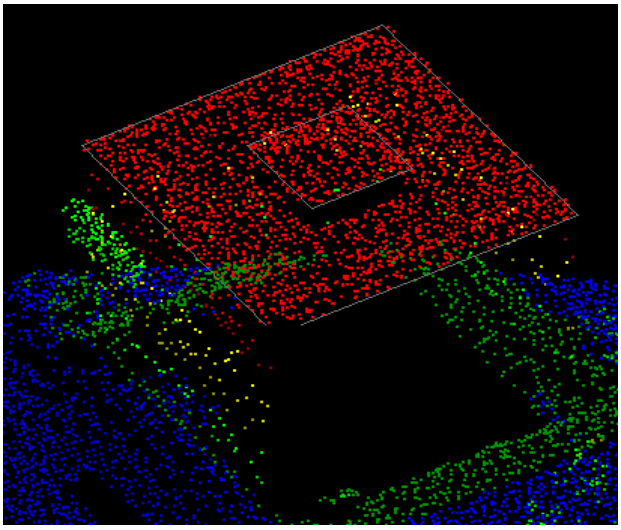

Figure 7. Points of one flattop plane

4. LABORATORY EXPERIMENT AND DISCUSSION

4.1 Laboratory experiment

Range biases and scan angle biases as mentioned in section 2 result to non-linear effect to the laser points position. The precision of range and scan angle for single laser point is analysed by laboratory experiment will help in reducing the effect and improving the performance of the ALS. The proposal method here repeats range measurement aiming to the same target through fixing the scan mirror. Rate of the laser instrument and scan mirror respectively are 35 kHz and 25 Hz. We select nine targets to test. 1355 point samples extracted from whole laser point sets are analysed statistically for each target. The specific details about the result of range are listed in Table 1 with R_{max} maximum range value, R_{min} minimum range value, R_{mean} mean range value, and STD_R standard deviations of range. Range resolved measurement precision is the standard deviation in the measured range data about the mean measured value.The corresponding shape of range

precision is shown as Fig.8. The mean of STD_R is 0.187 m. As can be seen from the table, the magnitude of range precision is outside the LiDAR precision specification (1 σ =2.5cm) under the target distance is less than 250m. So the range biases considered as a system error are introduced into the adjustment model.

Target	R_{max} (m)	R_{min} (m)	R_{mean} (m)	STD_R (m)
1	165.965	164.763	165.465	0.187
2	161.701	160.491	161.197	0.196
3	154.654	153.650	154.194	0.182
4	151.929	150.867	151.420	0.177
5	167.545	166.665	167.131	0.185
6	162.828	161.791	162.247	0.182
7	157.190	156.210	156.708	0.173
8	153.740	152.637	153.229	0.171
9	231.319	230.257	230.783	0.230

Table 1. Range results

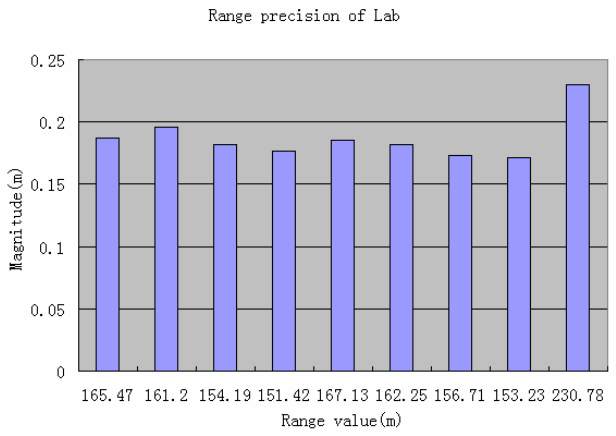

Figure 8. Magnitude of range precision for nine targets

The scan angle results are listed in Table 1 with A_{max} maximum scan angle value, A_{min} minimum scan angle value, A_{mean} mean scan angle value, and STD_A standard deviations of scan angle. The corresponding shape of scan angle precision is shown as Fig.9. The mean of STD_A is 0.00067° .The result demonstrate that scan angle measurement is so stable that scan angle errors as mention in section 2 can be omitted.

Target	A_{max} (degree)	A_{min} (degree)	A_{mean} (degree)	STD_A (degree)
1	1.402	1.397	1.400	0.00063
2	2.502	2.497	2.499	0.00071
3	3.701	3.697	3.699	0.00068
4	4.701	4.696	4.699	0.00069
5	1.401	1.397	1.399	0.00067
6	2.302	2.297	2.299	0.00063
7	3.601	3.597	3.599	0.00068
8	4.701	4.696	4.699	0.00069
9	-3.097	-3.102	-3.099	0.00064

Table 2. Scan angle results

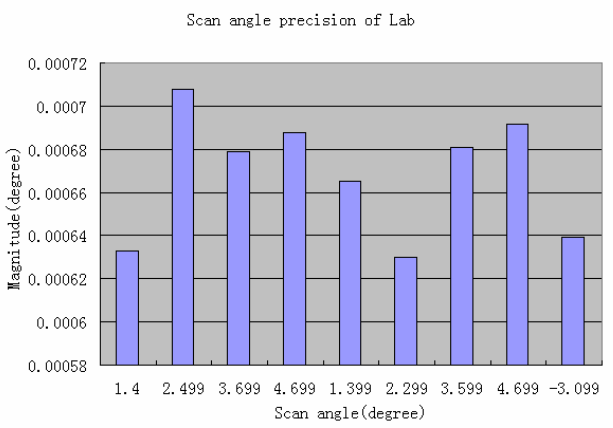

Figure 9. Magnitude of scan angle precision for nine targets

4.2 Discussion

The mention presented in paper enables the estimate the estimation of errors over general surfaces. No distinct landmarks are needed to perform the adjustment either as control or tie points. Consequently, there are only little restrictions on its application, as the adjustment model is based on modeling the actual effect of the error sources on the geo-reference of the laser point on the ground. A system based approach enables modeling and consequently removing the actual effect of the error sources. Furthermore, inclusion or elimination of error sources as more experience is gained becomes easier to implement. Error modeling concerns identifying the system errors and modeling their effect on the geo-reference of the laser point.

Least-squares offers a variety of possibilities for analyzing and testing the results. Tests can be performed to check if the residuals are randomly distributed, thus, if all systematic errors are removed. The estimated standard deviation of unit weight allows for proofing the correctness of the a priori assumptions for the observation accuracies. Measures for the internal and external reliability can be used for blunder detection and for accessing the geometry of the adjustment. They show how much single observations contribute to the estimation of the unknown parameters and how much a single observation is controlled by the other observations of the network. Blunders in the individual observations are not expected to be present, as they are detected during the plane search. However, the blunder detection in the laser point adjustment would reveal if planes used as tie-planes didn't match.

Re-processing the laser points with the corrections determined in the adjustment results in a geometrically correct point cloud of which the accuracy can be described by the standard deviations derived by error propagation. At each of the tie-planes the laser point accuracy can be verified, by computing the planes' normal vectors through the individual laser points. This gives the residuals in all three components x, y, z together with the length of the normal vector, i.e. the distance of the laser point to the plane.
Laboratory experiment is performed to analyse the range and scan angle performance aiming to the same target point. The magnitude of ranging precision and scan angle is computed. The ranging precision chiefly depends on the time measurement accuracy and the magnitude of S/N. The result can be considered as correction to the raw range-finder offset.

5. SUMMARY

This research studied the calibration of a laser altimeter system. The adjustment model presented enable modelling and removing the actual errors in laser point sets. By analyzing the properties of the proposed method, it has been demonstrated that moderate slopes are sufficient to generate reliable solutions. The only requirement consists in having the surface elements oriented in different directions. The compelling conclusion is that natural terrain will yield results that are accurate and reliable.

In addition to the effort of developing a robust method based on tie-planes, the extraction of other tie-features (e.g. lines) will be investigated. Finally, it is noted that in the case where aerial photographs are taken during an ALS mission, the ALS and photogrammetric observations can be processed together in one simultaneous block adjustment.

REFERENCES

Crombaghs, M., E. De Min and R. Bruegelmann (2000). On the Adjustment of Overlapping Strips of Laser Altimeter Height Data. International Archives of Photogrammetry and Remote Sensing, 33(B3/1): 230–237.

Filin, S., Vosselman, G., 2004. Adjustment of airborne laser altimetry strips. International Archives of Photogrammetry, Remote Sensing and Spatial Information Sciences 34 (Part B3), 285–289.

Huising, E. J. and L. M. Gomes Pereira (1998). Errors and accuracy estimates of laser data acquired by various laser scanning systems for topographic applications. ISPRS J. of Photogrammetry and Remote Sensing, 53(5): 245–261.

Lee, I., Schenk, T., 2001. Autonomous extraction of planar surfaces from airborne laser scanning data. In Proceedings of the Annual Conference of the American Society of Photogrammetry and Remote Sensing (ASPRS), St. Louis, MO, USA.

Lichti, D., 2004. A resolution measure for terrestrial laser scanners. International Archives of Photogrammetry, Remote Sensing and Spatial Information Sciences 34 (Part B5), 552–558.

Soininen,A., Burman,H., 2005. TerraMatch for MicroStation. Terrasolid Ltd, Finland.